Plasma Functionalized Surface of Commodity Polymers for Dopamine Detection

Georgina Fabregat,[a,b] Joaquin Osorio,[a] Alejandra Castedo,[b,c] Elaine Armelin,[a,b] Jorge J. Buendía,[a,b,c] Jordi Llorca,[b,c,*] and Carlos Alemán[a,b,*]

[a] *Departament d'Enginyeria Química, E. T. S. d'Enginyeria Industrial de Barcelona, Universitat Politècnica de Catalunya, Diagonal 647, 08028 Barcelona, Spain*

[b] *Center for Research in Nano-Engineering, Universitat Politècnica de Catalunya, Campus Sud, Edifici C', C/Pasqual i Vila s/n, Barcelona E-08028, Spain*

[c] *Institut de Tècniques Energètiques, E. T. S. d'Enginyeria Industrial de Barcelona, Universitat Politècnica de Catalunya, Diagonal 647, 08028 Barcelona, Spain*

[*] jordi.llorca@upc.edu and carlos.aleman@upc.edu

ABSTRACT

We have fabricated potentially generalizable sensors based on polymeric-modified electrodes for the electrochemical detection of dopamine. Sensitive and selective sensors have been successfully obtained by applying a cold-plasma treatment during 1-2 minutes not only to conducting polymers but also to electrochemically inert polymers, such as polyethylene, polypropylene, polyvinylpyrrolidone, polycaprolactone and polystyrene. The effects of the plasma in the electrode surface activation, which is an essential requirement for the dopamine detection when inert polymers are used, have been investigated using X-ray photoelectron spectroscopy. Results indicate that exposure of polymer-modified electrodes to cold-plasma produces the formation of a large variety of reactive species adsorbed on the electrode surface, which catalyze the dopamine oxidation. With this technology, which is based on the application of a very simple physical functionalization, we have defined a paradox-based paradigm for the fabrication of electrochemical sensors by using inert and cheap plastics.

Keywords: Conducting polymer; Dopamine; Plasma discharge; Polyethylene; Polythiophene; Surface activation

1. Introduction

Dopamine (DA), a member of the catecholamine family, acts as an important neurotransmitter in mammalian central nervous system modulating vital functions, such as voluntary movement. It is involved in motor and cognitive functions. In Parkinson's disease patients, DA releasing (dopaminergic) neurons in the central nervous system are dysfunctional or dying, causing a lack of dopamine in the target territories, which leads to impaired motor functions [1].

Among the potential methods developed for DA detection in the past decades, electrochemical techniques exhibit their predominance due to important advantages, such as rapid response, low cost and high sensitivity [2]. However, there are some limitations to measure DA under physiological conditions by common electrochemical methods. The main ones are related with the selectivity towards other species that coexist in the organism, such as ascorbic acid (AA) and uric acid (UA), which oxidize at almost the same potential that DA. Also, the detection of very low levels of DA (10 nM – 10 μM) represents a sensitivity challenge. Several strategies using, among others, nanocomposites [5,6], graphene [7,8], conducting polymers (CPs) [9-11], magnetic particles [12,13], or carbon natubes [14,15], have been reported in recent publications to overcome such problems. Another interesting strategy is the use of anionic ionomer-coated electrodes, which provides a way to increase the selectivity in the detection of DA, due to discrimination towards negatively charged species, such as the anionic forms of AA and UA [16,17]. Nevertheless, the development of these electrochemical sensors require a large number of steps for fabrication since application of the above mentioned compounds usually requires complex

chemical functionalization processes, incorporation of catalytic nanoparticles, processing of the nanocomposites, multi-step synthetic processes, etc [9-17].

The present study reports on the application of cold plasma technologies as a very simple and effective functionalization technique for the preparation of DA electrochemical sensors. More specifically, in this work we show that the treatment of polymeric surfaces in a room-temperature air-discharge plasma, which is a simple and powerful means of surface modification, enables the fabrication of DA sensors using not only electrochemically active CPs, as for example poly(3,4-ethylenedioxythiophene) (PEDOT) and poly(*N*-cyanoethylpyrrole) (PNCPy), but also conventional insulating and electrochemical inert polymers, as polypropylene, polyvinylpyrrolidone, polycaprolactone and polystyrene. Accordingly, plasma-based functionalization of polymer-coated electrodes have the potential be used and developed into truly selective and sensitive DA sensors, independently of the nature of the polymer, which is very attractive in terms of fabricating efficient but also cost-effective sensors.

2. Experimental

2.1. Materials

3,4-Ethylenedioxythiophene (EDOT), N-(2-cyanoethyl)pyrrole (NCPy), acetonitrile, anhydrous lithium perchlorate ($LiClO_4$), DA hydrochloride (3-hydroxytyramine hydrochloride), AA (L-configuration, crystalline), UA (crystalline) of analytical reagent grade were purchased from Sigma-Aldrich (Spain). All chemicals were used without further purification. Phosphate buffer solution (PBS) 0.1 M with pH= 7.4 was prepared as electrolyte solution by

mixing four stock solutions of NaCl, KCl, $NaHPO_4$ and KH_2PO_4. High-purity nitrogen was used for de-aeration of the prepared aqueous solutions.

2.2. Synthesis of conducting polymers

PEDOT and PNCPy (Scheme 1) films were prepared by choronoamperometry (CA) under a constant potential of 1.40 V [18] using a three-electrode two-compartment cell under nitrogen atmosphere (99.995% in purity) at 25 ºC. A bare glassy carbon electrode (GCE) with a diameter of 2 mm was used as working electrode while a steel AISI 316 sheet with an area of 1 cm^2 was employed as counter electrode. The surface of the GCE was polished with alumina powder and cleaned by ultrasonication prior to the deposition of the polymer. The reference electrode was an Ag|AgCl electrode containing a 3 M KCl aqueous solution.

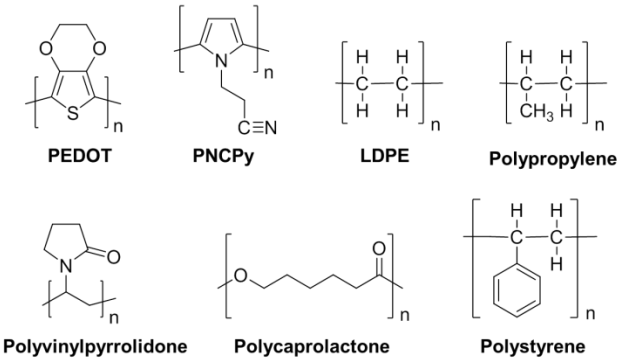

Scheme 1

All electrochemical experiments were conducted on a PGSTAT302N AUTOLAB potenciostat-galvanostat (Ecochimie, The Netherlands) equipped with the ECD module to measure very low current densities (100 μA-100 pA), which was connected to a PC computer controlled through the NOVA 1.6 software. PEDOT and PNCPy films were obtained using a 10 mM monomer

solution in acetonitrile with 0.1 M $LiClO_4$ and a polymerization time of 6 and 10 s, respectively.

2.3. Preparation of inert polymer-modified GCE

The following inter polymers were considered for this study (Scheme 1): low density polyethylene (LDPE), polypropylene, polyvinylpyrrolidone, polycaprolactone and polystyrene. Inert plastic-modified electrodes were prepared by depositing each plastic dissolved into an appropriate volatile solvent (*i.e.* chloroform, dichlorobenzene or methanol) onto GCE (*i.e.* solvent casting). Chloroform (10 mL) was used to dissolve 43 mg of polyvinylpyrrolidone, 46.5 mg of polycaprolactone and 33.5 mg of polystyrene, while dichlorobenzene (10 mL) was used to dissolve 34.4 mg of low density polyethylene (LDPE) and 52.4 mg of polypropylene. Polymer-modified GCEs were prepared by 6 μL of the corresponding polymer solution onto the GCE for solvent evaporation.

2.4. Cold plasma treatment

PEDOT-, PNCPy- and inert polymer-modified GCEs were prepared with a corona discharge in ambient atmosphere using a BD-20AC from Electro-Technic Products. The treatment of the polymers was performed using a Spring Tip wire electrode and a voltage of 45000 V at a frequency of 4.5 MHz. After plasma-treatment, modified GCE electrodes were used for DA detection experiments within 24 hours. Treatment with the nitrogen-plasma was performed using the same equipment and conditions with the obvious exception that the corona discharge was conducted in a nitrogen atmosphere. This inert atmosphere was created through a continuous nitrogen flow. After finishing

the treatment with nitrogen plasma, material were exposed to air for characterization and electrochemical measurements.

2.5. Electrochemical measurements for DA detection

Electrochemical detection was carried out by cyclic voltammetry (CV) using the Autolab PGSTAT302N equipment described above. All electrochemical experiments were performed in a glass cell containing 10 mL of PBS 0.1 M (pH=7.4) at room temperature and equipped with saturated Ag|AgCl as reference electrode and platinum (Pt) wire as counter electrode. Voltammograms were recorded in the potential range from -0.40 to 0.80 V at a scan rate of 50 $mV \cdot s^{-1}$ unless other scan rate is explicitly specified. All the modified electrodes were in contact with the electrolyte solution for 5 min prior to CV measurements.

2.6. FTIR and scanning electron microscopy (SEM)

IR absorption spectra were recorded on a FTIR Jasco 4100 spectrophotometer. Samples were placed in an attenuated total reflection accessory (Top-plate) with a diamond crystal (Specac model MKII Golden Gate Heated Single Reflection Diamond ATR). For each sample 32 scans were performed between 4000 and 600 cm^{-1} with a resolution of 4 cm^{-1}.

The surface morphology of untreated and plasma treated samples was examined by SEM. Samples were mounted on a double-side adhesive carbon disc and sputter-coated with a thin layer of carbon to prevent sample charging problems. Microscopy studies were carried out using a Focused Ion Beam Zeiss Neon40 scanning electron microscope equipped with an energy dispersive X-Ray (EDX) spectroscopy system and operating at 5 kV.

2.7. X-ray photoelectron spectroscopy (XPS)

XPS assays were performed on a SPECS system equipped with an Al anode XR50 source operating at 150 mW and a Phoibos MCD-9 detector. The pressure in the analysis chamber was always below 10^{-7} Pa. The pass energy of the hemispherical analyzer was set at 25 eV and the energy step was set at 0.1 eV. Data processing was performed with the CasaXPS program (Casa Software Ltd., UK). The binding energy (BE) values were referred to the C 1s peak at 284.8 eV. Atomic fractions were calculated using peak areas normalized on the basis of acquisition parameters after background subtraction, experimental sensitivity factors and transmission factors provided by the manufacturer.

3. Results and Discussion

3.1. Conducting polymer-based sensors: Effect of the surface treatment time

Although the ability of PEDOT and PNCPy films to detect DA was examined in previous works [11,19,20], we briefly re-investigate this topic to illustrate more clearly the effects of the functionalization with cold plasma in the detection process. The response of the two CPs against DA was found to be radically different (Figure 1a). Thus, selective and simultaneous detection of DA, UA and AA using PNCPy is difficult because oxidation peaks are weak and partially overlapped while, in opposition, oxidation peaks are well resolved when employing PEDOT electrodes.

On the other hand, the surface of PEDOT- and PNCPy-modified GCEs was treated with cold plasma for functionalization (*i.e.* corona discharge at 0.5 J cm^{-2}

during 2 min). Figure 1 compares the voltammetric response of untreated and plasma-functionalized electrodes for detection assays of DA, UA and AA (100 μM each). Voltammograms recorded using bare GCEs have been included for comparison. Although plasma treatment provokes a significant reduction of the reversal peak intensity at 0.70 V for all systems, it is worth noting that this effect is relatively small for the anodic intensities associated to the oxidation of the three analytes. Furthermore, both plasma-functionalized PNCPy and PEDOT electrodes are able to selectively detect the oxidation of DA, UA and AA, while untreated PNCPy is unable to selectively discriminate among them. Regarding to the bare GCE, it is not able to selectively detect the presence of AA in the mixture, independently of the plasma treatment. The sensitivity and resolution parameters, which have been expressed as the ratio between the peak intensity for the oxidation of a given species and its concentration in the mixture (μA/mM) and the difference between the peak oxidation potentials of the two species (V), respectively, for untreated and plasma treated PEDOT- and PCNPy-modified electrodes are listed in Table 1.

In the case of plasma-functionalized electrodes small, or even imperceptible, shoulders have been identified in some voltammograms (marked with grey arrows in Figure 1b). These shoulders, which are shifted with respect to identified oxidation peaks, have been associated with secondary oxidation processes of AA (PNCPy, PEDOT and bare GCE) or UA (only PNCPy) eventually catalysed by non-predominant reactive species created during the cold-plasma treatment. On the other hand, the chronoamperometric response of the plasma-functionalized electrodes upon the successive addition of DA is the one expected for conventional potentiometric sensors. More specifically, the injection of DA

caused a rapid enhancement of the current, which increased steeply to reach a stable value (not shown).

The DA detection limit of PEDOT- and PNCPy-modified GCEs with cold-plasma treatment was derived from the variation of the anodic peak intensity (i_p), as determined by CV, against the DA concentration. The resulting calibration curve (Figure 2a) evidences a linear behavior in the whole interval of examined DA concentration (from 0.5 to 100 μM DA). The detection limit expressed as $3.3 \cdot \sigma / S$, where σ and S is the standard deviation of the response and the slope of the calibration curve for DA concentrations ranging from 0.5 to 5 μM (inset of Figure 2a) is 140 and 750 nM for PEDOT and PNCPy, respectively. These values are significantly lower than those obtained for non-functionalized samples [11,20], evidencing an improvement not only in the resolution (especially for PNCPy) but also in the sensitivity. Comparison with sophisticated carbon-based materials recently developed to detect DA, as for example those based on graphene oxide [21,22], also reveals the good performance of the simple plasma-functionalized electrodes described in this work. Zhang and co-workers used graphene oxide–carbon nanotubes [21] and reduced graphene oxide-poly(para-phenylenediamine) [22] hybrids to achieve a detection limit of 40 nm and 360 nm, respectively. The DA detection limit of reduced graphene oxide sheets is 200 μM when organized in simple sheets [23], decreasing up to 170 nm when it is prepared as a 3D material using spherical templates [24].

The cold plasma technique has a remarkable effect on the surface modification of CP films, enhancing their selectivity, sensitivity, and the interval with a linear behavior in the DA detection. This advantageous response could be attributed to the surface polarity, cross-layer linking and other microstructural changes induced by the plasma, which influence the DA sensing properties. Accordingly, an important issue may be the

influence on the effective DA detection that has the time that plasma power is applied (t_{cp}). In order to investigate the effect of the surface treatment time, PEDOT-modified GCEs were treated considering different t_{cp} values (*i.e.* from 15 to 120 s). Figure 2b compares the voltammograms of 100 μM DA in 0.1 M PBS at these functionalized electrodes. The influence of t_{cp} in the oxidation peak potential is null (E= 0.176 V in all cases). Similarly, the influence of t_{cp} in the anodic peak intensity (i_p) is very small (Figure S1), growing from 1.50 μA for t_{cp}= 15 s to 1.63 μA for t_{cp}= 120 s. Accordingly t_{cp} is not a crucial factor for the detection process once it is higher than 15 s.

3.2. Proof of concept: Polyethylene-based sensors

Results obtained in the previous sub-section evidence that the application of the plasma treatment to CPs induces the formation of very active species that improve the sensing response of the initial materials. As a probe of concept, it would be interesting to ascertain if such physical treatment enables the functionalization of an electrochemically inactive polymer, such as low density polyethylene (LDPE), transforming it into an electroactive material suitable for the fabrication of very cheap electrochemical sensors. For this purpose, LDPE sensors were manufactured by solvent casting onto GCE substrate. Comparison of the FTIR spectra recorded for LDPE films without and with cold-plasma treatment (Figure S2) indicates the apparition of some bands, which has been attributed to the formation of reactive species at the surface, as corroborated by XPS analyses (see below).

For the LDPE-modified GCE without cold-plasma treatment, the cyclic voltammogram recorded in a solution of 0.1 M PBS with 1 mM DA does not provide any oxidation peak (Figure 3a), indicating that, as expected, LDPE is not able to detect such neurotransmitter. In contrast, the voltammogram recorded using an identically

fabricated electrode but applying a cold-plasma treatment during 1 min, shows a sharp oxidation peak at 0.20 V that corresponds to the DA (Figure 3a). Considering that the DA concentration estimated in the synapse is 1.6 mM, this result corroborates that efficient detectors can be fabricated by combining an organic matrix with a simple air-plasma treatment. Furthermore, this detector is stable since it only decreases ~1.7 μA (~10%) after three consecutive oxidation-reduction cycles (*i.e.* detection cycles).

Additional assays with cold-plasma treated LDPE-modified GCEs were performed using 100, 10 and 1 μM DA concentrations (Figure 3b). Results indicate that the oxidation of DA molecules was detected as a clear oxidation peak for the 100 μM solution (i_p= 0.33 μA), as a weak shoulder for the 10 μM solution (i_p= 0.07 μA). Because of their simplicity, these electrodes are very promising for the detection of the neurotransmitter. Thus, it should be remarked that the limit for the electrochemical detection of DA at sophisticated 3-layered films made of PEDOT (external and internal layers) and poly(N-methylpyrrole) (intermediate layer to create a dielectric effect) coated with AuNPs at the external layer was 2 μM [11], while the limit at a GCE coated with a CP especially designed to detect DA, poly(hydroxymethyl-3,4-ethylenedioxythiophene), was slightly higher [19].

Table 1 compares the sensitivity and resolution obtained for the determination of DA, AA and UA using plasma treated LDPE-modified electrodes with those achieved using PEDOT- and PNCPy-modified electrodes. As it can be seen, the oxidation peaks of the three analytes are similarly resolved for the three plasma treated polymer-modified electrodes. Thus, the sensitivity of treated LPDE is similar to that of treated CPs. The stability and reproducibility of plasma treated PEDOT- and LDPE-modified electrodes is demonstrated in Figure 4, which represents the variation of the peak intensity and peak potential against the number of detection cycles using 100 μM DA in

PBS. As it can be seen, the variation of the potential with the number of consecutive detection cycles is practically null, whereas the peak intensity decreases slowly. Both features reflect the very significant stability of the sensors. Furthermore, the relatively low standard deviations observed in the peak intensities prove the reproducibility of the plasma treated.

On the other hand, comparison of the response against 100 μM DA of plasma-functionalized LDPE films of different thickness suggested that the detection process is mainly a surface phenomenon. More specifically, the i_p values determined for plasma treated LDPE films of 447±39 and 202±27 nm thickness, which were prepared by dissolving 34.4 and 17.2 mg of polymer in 10 mL of chloroform and depositing 6 μL of such solution onto the GCEs, were very similar (0.33 to 0.26 μA, respectively).

3.3. Extension to other electrochemically inert polymers

The successful and unexpected results displayed in the previous sub-section for LDPE, led us to extend the applicability of the proposed approach to manufacture effective DA sensor to other inert polymer-modified GCEs. Figure 5 shows the voltammograms recorded in a 0.1 M PBS solution with 10 μM DA at cold-plasma treated polypropylene-, polyvinylpyrrolidone-, polycaprolactone- and polystyrene-modified GCEs. A clear oxidation peak is observed in all cases, the value of the anodic peak intensity depending on the chemical nature of the inert polymer. Moreover, the i_p for all such inert polymer-modified GCEs is higher than that of the LDPE-modified GCE (Figure S3). Indeed, the i_p for one of such polymers, polycaprolactone, was higher than that of PEDOT. The oxidation peak potential, *E*, remains comprised between 0.171 and 0.184 V in all cases (Figure S4).

The overall of these results indicate that electrochemically inert polymers can be successfully transformed into electrochemical sensors for DA detection by functionalizing through a simple cold-plasma treatment. The implications of this approach are very significant. The replacement of CPs and inorganic catalytic nanoparticles by conventional commodity polymers provokes a significant reduction in the economic cost of the detection devices. Also, the substitution of nanocomposites processing and/or multi-step synthetic processes by a simple cold-plasma treatment results in a significant diminution of the cost. Furthermore, this strategy is friendly from an environmental point of view since it opens a new door for the technological reuse of recycled polymers.

3.4. Detection mechanism: Effect of the plasma on the polymeric surfaces

Owing to the surface character of the processes involved, we have studied the functionalization of the surfaces of the electrodes by the air plasma treatment using XPS. We have used bare glassy carbon (GC) rods and GC rods modified at the surface with PEDOT and LDPE as prepared and after plasma treatment of different duration. Two or three fresh samples for each electrode were analysed and no significant variations were encountered. Table 2 compiles the surface composition determined by XPS on an atomic basis.

The spectrum recorded over the bare GC substrate as prepared shows the presence of C and O and a minor contribution of N. This is in accordance with the reported structure of GC, where phenol, carbonyl, carboxyl, lactone and quinone functional groups are present [25]. The spectrum of the electrode functionalised with PEDOT shows a larger amount of O and the presence of S according to its structure, whereas almost no N is

present on the surface. As expected, the spectrum recorded over the electrode functionalised with LDPE has the highest amount of C.

Upon plasma treatment, the surfaces of the electrodes get enriched in O and N in all cases, as it is reflected by the plots of the C/O and C/N atomic ratios (Figure S5). These graphs and the values reported in Table 2 allow us to conclude that an important enhancement of both O and N occurs as a direct consequence of the plasma treatment. This is in agreement with previous reports in the literature concerning carbon materials exposed to O_2 and N_2 plasmas [26-28].

The C 1s, O 1s and N 1s spectra of untreated and plasma-functionalized (t_{cp}= 1 min) bare GC are displayed in Figure 6. The analysis of the C 1s signal reveals the presence of different surface species both before and after plasma treatment. The main bands at 285.5 and 286.3 eV can be attributed to Csp^2 and Csp^3 species, respectively, whereas those at higher binding energies are ascribed to several C–O and C–N species. After plasma treatment the amount of C sp^3 species decreases. The same trend is observed in the O 1s spectra, where the intensity of the O–Csp^2 component at 533.1 eV increases after plasma treatment. Concerning the N 1s spectra, it is clear that new N–bearing species are formed upon exposure to plasma; in particular the new band at 407.8 eV corresponds to nitrate species. Bands at 398.5, 400.3 and 403.7 eV are ascribed to pyridinic, pyrrolic and quaternary nitrogen species. The spectra recorded after 2 min plasma is virtually identical to those recorded after 1 min plasma.

The C 1s, O 1s, N 1s and S 2p spectra of as prepared and plasma treated (t_{cp}= 1 and 2 min) PEDOT-modified GC samples are provided in Figure 7. Initially, the C 1s spectrum shows the presence of the polymer by an increase of the Csp^3 signal with respect to the Csp^2 signal present in the C 1s spectrum of the GC support. In addition, the S 2p spectrum shows the presence of sulphur species according to the structure of

PEDOT. The progressive air plasma treatment for t_{cp} = 1 and 2 min allows for a monitoring of the surface changes. Besides, there is an increase of intensity of the bands at 288.3 and 290.0 eV in the C 1s spectra, which correspond to highly oxidised carbon such as carboxylate groups. This is particularly important in the sample treated with plasma for t_{cp}= 2 min. A similar change is observed in the O 1s spectra, where the contribution of oxygen at high binding energies increases. On the other hand, the sulphur species in PEDOT change completely into sulphite and sulphate species at 169-170 eV, respectively. The effect of plasma is clear here since the S signal decreases in intensity and simultaneously strongly oxidizes. Finally, the N spectra also change drastically upon exposure to plasma, where the band at 407.3 eV that appears after 1 min plasma corresponds to nitrate species and that at 404.1 eV observed after 2 min corresponds to nitrite species, again pointing to a strong oxidation of the surface. Therefore, in this case the plasma treatment duration determines the abundance and nature of the resulting species adsorbed at the surface.

The C 1s, O 1s and N 1s spectra of the untreated and plasma-treated (t_{cp}= 30 s, 1 min and 2 min) GC-modified PE samples are shown in Figure S6. In this case, the duration of the plasma treatment seems less important and the spectra obtained after 30 s, 1 min and 2 min are fairly similar. Regarding carbon species, the main transformation observed in this case is the decrease of Csp^2 species. The spectra of O and N show an increase of oxidized species in both cases, as in the case of the PEDOT sample. These observations are in good agreement with previous results on plasma-functionalized LDPE [29,30], which also reported that oxidized species are introduced by the plasma treatment.

It is shown that exposure of the electrodes to air plasma leads to the formation of a large variety of species adsorbed on their surface, which is attributed to the high

reactivity of excited species formed in the plasma, such as N, O, N_2^+, O_2^+ and O^+. According to literature, these plasma species are able to break the ordered structure of carbon assemblies, favouring substitution reactions, breaking aromaticity and generating defects and aliphatic fragments [31]. Furthermore, these species are clearly different for unmodified and polymer-modified GC, which support the detection results.

Accordingly, the plasma exposure induces functionalization of the polymeric surface. The interaction of the polymer surface with the plasma can cause hydrogen separation from polymeric chains and free radical creation. Thus, the functionalization arises from the surface exposure to air and reactive species previously adsorbed by the polymeric matrix. The radicals created by the plasma activation interact with oxygen and nitrogen and, thus, new functional groups are incorporated into the polymer surface that becomes very active. XPS results clearly indicate that the nature of reactive species formed upon exposure of the polymer-modified electrode to the cold plasma depends on the chemical structure of the polymer and, in some cases, on the duration of the treatment.

The oxidation of DA at the plasma treated polymer-modified GCEs demonstrates the electrocatalytic role of the plasma activated surfaces. Considering that reactive species at the surface catalyse the transformation of DA to its oxidized form dopamine-*o*-quinone (DQ), differences in the response of the different plasma-treated polymers should be attributed to the diversity of reactive species at the treated-electrode surface. More specifically, the chemical nature of the reactive species affects the capacity of the surface to exchange electrons with the surrounding environment. Thus, the oxidation of DA to DQ follows a relatively simple electron transfer mechanism: DA first diffuses onto the plasma treated polymer-modified electrode and releases electrons, which are accepted by the working electrode while forming DQ. In the reverse scan DQ captures electrons from the electrode to form DA. Similarly, changes in the selective detection of

three analytes (AA, DA and UA) between functionalized and unfunctionalized CPs should be attributed to differences in the catalytic role played by the formed reactive species in the oxidation of each analyte.

The mechanism derived from XPS results is fully consistent with the plasma-induced changes in the surface morphology. Figure 8 compares SEM micrographs of untreated and plasma treated samples of PEDOT and PNCPy-modified GCEs. Untreated samples exhibit a relatively compact morphology . More specifically, untreated PEDOT consists on both sheets and sticks that aggregate forming a homogeneous distribution of narrow and tortuous pores (Figure 8a, left), which play a crucial role in the electrochemical properties of PEDOT, facilitating the mobility of dopant ions in oxidation and reduction processes (*i.e.* access and escape of ions into / from the polymer matrix, respectively). Besides, PNCPy presents an extremely compact surface without pores (Figure 8b, left) that is in agreement with its poor electrochemical performance. The compact morphologies of two untreated CPs transform into porous networks after plasma application (Figure 8, right). In the case of PEDOT, chemical processes induced by the application of plasma cause the collapse of sheets and sticks, giving place to the formation of abundant pores that are much wider than those observed untreated samples. Moreover, the tortuosity of the pores is also lost due to such molecular redistribution, which facilitates the diffusion of DA molecules and, therefore, the effectivity of the electron transfer process discussed above. For PNCPy, the extremely compact surface becomes porous after plasma treatment, which is consistent with enhancement of the electrochemical response. These features combined with the formation of reactive species explain the DA detection of plasma-treated polymer-modified electrodes.

3.5. Dependence on plasma atmosphere and electrode substrate.

The effect of the plasma atmosphere in the formation of electrochemically active compounds was examined by comparing the performance of LDPE-modified GCE functionalized using air- and nitrogen-plasma (*i.e.* oxidizing and inert atmospheres, respectively). Comparison of the response for the detection of 10 μM DA indicates that the influence of the plasma atmosphere is relatively small (Figure 9a). Thus, the anodic peak intensity and the oxidation potential are practically the same for both plasma-functionalized electrodes. These results, which are fully consistent with the early observations of Behnisch *et al.* [32] for LDPE surfaces treated with nitrogen and oxygen plasma, evidence a determining influence of oxygen residues in the nitrogen plasma. Overall, these observations together with the XPS measures suggest that plasma functionalization provokes the formation of very reactive and unstable species. In the case of nitrogen plasma the oxygen required from to the formation of some of such species comes from the own plastic (*i.e.* adsorbed oxygen) or from the atmosphere once the nitrogen flow is retired and the material is exposed to the atmosphere.

On the other hand, untreated GCEs were combined with plasma-functionalized LDPE to examine the influence of the functionalization of the electrode substrate on the DA detection. Although these experiments were extremely difficult because of lack of adherence between the bare GCE and the plasma-treated LDPE, satisfactory electrodes were finally obtained by pressing the latter onto the former. As it can be seen, the electrochemical response against a solution with DA, UA and AA (100 μM each) does not depend on the formation of reactive species at the surface of the GCE substrate (Figure 9b). Furthermore, the influence on the sensitivity is very small, even though there is a reduction on the resolution between DA and AA (Table 1). However, the simultaneous functionalization of the inert plastic and the electrode substrate provides

an important advantage: the plasma-induced degradation products combine at the plastic/GCE interface combine favoring the adherence between the two components.

4. Conclusions

Application during 1-2 min of air-plasma to polymeric films coating CGEs has been found to result in sensors with resolution and sensitivity similar to those achieved through sophisticated chemical modifications. This simple and successful procedure can be applied not only to CPs but also to electrochemically inert and cheap commodity plastics. The electrochemical response of the plasma-functionalized materials has been explained by the high reactivity of the simple excited species observed on the surface, which have electrocatalytic effects in the oxidation DA. The present study has opened a facile, simple and rapid way for the fabrication of sensitive DA detectors that can be implemented as a very cost-effective diagnostic test.

Acknowledgements

Authors acknowledge MINECO/FEDER (MAT2015-69367-R) for financial support. G.F. is thanked for the financial support through a postdoc-UPC. J.L. is Serra Húnter Fellow. J.L. and C.A. are grateful to ICREA Academia program.

References

[1] M. Politis, O. Lindvall, Clinical application of stem cell therapy in parkinson's disease, BMC Med. 10 (2012) 1–7.

[2] E. Seeman, H. B. Niznik, Dopamine receptors and transporters in parkinson's disease and schizophrenia, FASEB J. 4 (1990) 2737–2744.

[3] S. Nikolaus, C. Antke, H. W. Müller, In vivo imaging of synaptic function in the central nervous system: I. Movement disorders and dementia, Behav. Brain Res. 204 (2009) 1–31.

[4] K. Jackowska, P. Krysinski, New trends in the electrochemical sensing of dopamine, Anal. Bioanal. Chem. 405 (2013) 3753–3771.

[5] L. A. Mercante, A. Pavinatto, L. E. O. Iwaki, V. Zucolotto, O. N. Oliveira, L. H. C. Mattoso, D. S. Correa, Electrospun polyamide 6/poly(allylamine hydrochloride) nanofibers functionalized with carbon nanotubes for electrochemical detection of dopamine, ACS Appl. Mater. Interfaces 7 (2015) 4784–4790.

[6] A. K. Yang, Y. Xue, Y. Zhang, X. F. Zhang, H. Zao, X. J. Li, Y. J. He, Z. B. Yuan, A simple one-pot synthesis of graphene nanosheet/SnO_2 nanoparticle hybrid nanocomposites and their application for selective and sensitive electrochemical detection of dopamine, J. Mater. Chem. B 1 (2013) 1804–1811.

[7] X. M. Feng, Y. Zhang, J. H. Zhou, Y. Li, S. F. Chen, L. Zhang, Y. W. Ma, L. H. Wang, X. H. Yan, Three-dimensional nitrogen-doped graphene as an ultrasensitive electrochemical sensor for the detection of dopamine, Nanoscale 7 (2015) 2427–2432.

[8] S. Pruneanu, A. R. Biris, F. Pogacean, C. Socaci, M. Coros, M. C. Rosu, F. Watanabe, A. S. Biris, The influence of uric and ascorbic acid on the electrochemical detection of dopamine using graphene-modified electrodes, Electrochim. Acta 154 (2015) 197–204.

[9] C. L. Weaver, H. Li, X. Luo, X. T. Cui, A graphene oxide/conducting polymer nanocomposite for electrochemical dopamine detection: Origin of improved sensitivity and specificity, J. Mater. Chem. B 2 (2014) 5209–5219.

[10]M. Martí, G. Fabregat, F. Estrany, C. Alemán, Nanostructured conducting polymer for dopamine detection, J. Mater. Chem. 20 (2010) 10652–10660.

[11]G. Fabregat, E. Armelin, C. Alemán, Selective detection of dopamine combining multilayers of conducting polymers with gold nanoparticles, J. Phys. Chem. B 118 (2014) 4669–4682.

[12]Z. Herrasti, F. Martinez, E. Baldrich, Electrochemical detection of dopamine using streptavidin-coated magnetic particles and carbon nanotube wiring, Sens. Actuators B 203 (2014) 891–898.

[13]G. Lai, Y. Liu, A. Yu, D. Han, H. Zhang, Simultaneous sensitive determination of dopamine and uric acid in the presence of excess ascorbic acid with a magnetic chitosan microsphere/thionine modified electrode, Anal. Lett. 46 (2013) 1525–1536.

[14]V. Vinoth, J. J. Wi, A. M. Asiri, S. Anandan, Simultaneous detection of dopamine and ascorbic acid using silicate network interlinked gold Nanoparticles and multi-walled carbon nanotubes, Sens. Actuators B 210 (2015) 731–741.

[15]X. M. Fei, J. Luo, R. Liu, J. C. Liu, X. Y. Liu, M. Q. Chen, Multiwalled carbon nanotubes noncovalently functionalized by electro-active amphiphilic copolymer micelles for selective dopamine detection, RSC Adv. 5 (2015) 18233–18241.

[16]L. S. Rocha, H. M. Carapuça, Ion-exchange voltammetry of dopamine at nafion-coated glassy carbon electrodes: Quantitative features of ion-exchange partition and reassessment on the oxidation mechanism of dopamine in the presence of excess ascorbic acid, Bioelectrochemistry 69 (2006) 258–266.

[17]Chou, J.; T. J. Ilgen, S. Gordon, A. D. Ranasinghe, E. W. McFarland, H. Metiu, S. K. Buratto, Investigation of the enhanced signals from cations and dopamine in electrochemical sensors coated with nafion J. Electroanal. Chem. 632 (2009) 97–101.

[18]C. Ocampo, R. Oliver, E. Armelin, C. Alemán, F. Estrany, Electrochemical synthesis on steel electrodes of poly(3,4-ethylenedioxythiophene): Properties and characterization, J. Polym. Res. 13 (2006) 193–200.

[19]G. Fabregat, J. Casanovas, E. Redondo, E. Armelin, C. Alemán, A rational design for the selective detection of dopamine using conducting polymers, Phys. Chem. Chem. Phys. 16 (2014) 7850–7861.

[20]G. Fabregat, E. Córdova-Mateo, E. Armelin, O. Bertran, C. Alemán, Ultrathin films of polypyrrole derivatives for dopamine detection, J. Phys. Chem. C 115 (2011) 14933–14941.

[21] Y. Zhang, Y. Ji, Z. Wang, S. Liu, T. Zhang, Electrodeposition synthesis of reduced graphene oxide–carbon nanotube hybrids on indium tin oxide electrode for simultaneous electrochemical detection of ascorbic acid, dopamine and uric acid, RSC Adv. 5 (2015) 106307–106314.

[22] S. Liu, B. Yu, T. Zhang, Preparation of crumpled reduced graphene oxide–poly(p-phenylenediamine) hybrids for the detection of dopamine, J. Mater. Chem. A 1 (2013) 13314–13320.

[23] Y. Wang, Y. Li, L. Tang, J. Lu, J. Li, Application of graphene-modified electrode for selective detection of dopamine, Electrochem. Commun. 11 (2009) 889–892.

[24] B. Yu, D. Kuang, S. Liu, C. Liu, T. Zhang, Template-assisted self-assembly method to prepare three-dimensional reduced graphene oxide for dopamine sensing, Sens. Actuators B 205 (2014) 120–126.

[25]J. L. Hueso, J. P. Espinos, A. Caballero, J. Cotrino, A. R. Gonzalez-Elipe, XPS investigation of the reaction of carbon with NO, O_2, N_2 and H_2O plasmas, Carbon 45 (2007) 89–96.

[26]T. Xu, J. Yang, J. Liu, Q. Fu, Surface modification of multi-walled carbon nanotubes by O_2 plasma, Appl. Surf. Sci. 253 (2007) 8945–8951.

[27]O. M. Ba, P. Marmey, K. Anselme, A. C. Duncan, A. Ponche, Surface composition XPS analysis of a plasma treated polystyrene: Evolution over long storage periods, Colloids Surf. B Biointerfaces 145 (2016) 1–7.

[28]K. Wang, J. Li, C. S. Ren, D. Z. Wang, Y. N. Wang, Surface modification of polyethylene (PE) films using dielectric barrier discharge plasma at atmospheric pressure, Plasma Sources Sci. T. 10 (2008) 433–437.

[29]R. Foerch, G. Kill, M. J. Walzak, "Plasma surface modification of polyethylene: Short term vs. long term plasma treatment". In "Plasma surface modification of polymers", Strobel, M.; Lyons, C.; Mittal, K. L. (Eds), pp 99–111. VSP, 1994.

[30]M. Pascual, R. Sanchis, L. Sánchez, D. García, R. Balart, Surface modification of low density polyethylene (LDPE) film using corona discharge plasma for technological applications, J. Adhes. Sci. Technol. 22 (2008) 1425–1442.

[31]J. Yang, G. Mestl, R. Schlögl, J. Find, Reaction of NO with carbonaceous materials: 1. Reaction and adsorption of NO on ashless carbon black, Carbon 38 (2000) 715-727.

[32]J. Behnisch, A. Hollander, H. Zimmermann, Surface modification of polyethylene by remote dc discharge plasma treatment, J. Appl. Polym. Sci. 49 (1993) 117–124.

Table 1. Sensitivity and resolution obtained for the determination of DA, AA and UA in 0.1 M PBS using different untreated and plasma treated polymer modified electrodes.

	Sensitivity (μA/mM)			**Resolution (V)**	
	DA	**AA**	**UA**	**AA-DA**	**UA-DA**
PEDOT	46.3	25.4	71.6	0.196	0.113
PEDOT (plasma)	30.8	6.3	31.7	0.131	0.137
PNCPy	51.2	-	51.2	-	0.000
PNCPy (plasma)	26.7	4.8	31.2	0.142	0.137
LDPE	-	-	-	-	-
LDPE (plasma)[a]	26.4	4.8	25.7	0.135	0.118
LDPE (plasma)[b]	14.6	9.7	11.4	0.066	0.137

[a] Plasma treatment was applied on LDPE-modified GCEs. [b] Plasma treatment were applied on LDPE films, which were subsequently immobilized on untreated bare GCEs by applying pressure.

Table 2. Atomic percent composition of untreated (as prepared) and air-plasma (t_{cp}= 1 and 2 min) of treated bare GCE, and both PEDOT- and LDPE-modified GCE. For the latter, samples treated using t_{cp}= 30 s were also considered.

		atomic %			
		C	O	N	S
GCE	as prepared	73.6	25.0	1.4	-
	plasma 1 min	61.3	35.3	3.4	-
	plasma 2 min	64.5	32.1	3.4	-
PEDOT	as prepared	60.1	35.8	0.8	3.3
	plasma 1 min	59.0	37.4	3.1	0.5
	plasma 2 min	44.0	49.9	4.0	2.1
LDPE	as prepared	77.2	22.3	0.5	-
	plasma 30 s	63.8	33.5	2.7	-
	plasma 1 min	67.1	31.0	1.9	-
	plasma 2 min	68.4	29.5	2.1	-

CAPTIONS TO FIGURES

Figure 1. Control voltammograms of DA, UA and AA (100 μM each) in 0.1 M PBS at (a) untreated and (b) air-plasma treated bare GCE, and both PNCPy- and PEDOT-modified GCE. Grey arrows in (b) indicate secondary oxidation processes (see text). Scan rate: 100 mV/s.

Figure 2. (a) DA detection limit of PEDOT- and PNCPy-modified GCEs with cold-plasma treatment, as obtained from the standard addition of 10 μL of DA to 10 mL of 0.1 M PBS. The anodic peak intensity (i_p) was determined by CV using a scan rate of 50 $mV \cdot s^{-1}$. (b) Control voltammograms of 100 μM DA in 0.1 M PBS at cold-plasma treated PEDOT-modified GCE prepared using different t_{cp} values. Scan rate: 100 mV/s.

Figure 3. (a) Control voltammogram of 1 mM DA in 0.1 M PBS at LDPE-modified GCE. Voltammograms recorded using untreated electrodes (black) and cold-plasma treated electrodes (red: first detection cycle; blue: third detection cycle). (b) Control voltammograms of 100, 10 and 1 μM DA at cold-plasma treated LPDE-modified GCEs. Right: complete voltammograms; Left: magnification of the region associated to the oxidation of DA molecules. In all cases: scan rate: 100 mV/s. Initial and final potentials: -0.40 V; reversal potential: +0.80 V.

Figure 4. Variation of the peak intensity (filled diamonds) and peak potential (empty squares) against the number of consecutive detection cycles of 100 μM DA using plasma treated (a) PEDOT- and (b) LDPE-modified electrodes. All experiments were performed in quadruplicate using independent electrodes. Error bars correspond to the standard deviations of independent measures.

Figure 5. Control voltammogram of 10 μM DA in 0.1 M PBS at (a) polypropylene-, (b) polyvinylpyrrolidone-, (c) polycaprolactone- and (d) polystyrene-modified GCE. Voltammograms recorded using untreated electrodes (dashed lines) and cold-plasma

treated electrodes (solid line) are displayed in all cases. Scan rate: 100 mV/s. Initial and final potentials: -0.40 V; reversal potential: +0.80 V.

Figure 6. C 1s, O 1s and N 1s XPS spectra of bare glassy carbon as prepared (left) and after 1 min plasma (right).

Figure 7. C 1s, O 1s, N 1s and S 2p XPS spectra of PEDOT untreated (left) and after plasma-treatment using t_{cp}= 1 min (center) and t_{cp}= 2 min (right).

Figure 8. SEM micrographs of (a) PEDOT and (b) PNCPy before (left) and after (right) plasma treatment using t_{cp}= 2 min.

Figure 9. (a) Control voltammograms of 10 µM DA in 0.1 M PBS at air- and nitrogen-plasma treated LPDE-modified GCEs. (b) Control of 100 µM DA, 100 µM UA and 100 µM AA in 0.1 M PBS in 0.1 M PBS at plasmas-functionalized LPDE pressed onto a bare untreated GCE. In all cases: scan rate: 100 mV/s. Initial and final potentials: -0.40 V; reversal potential: +0.80 V.

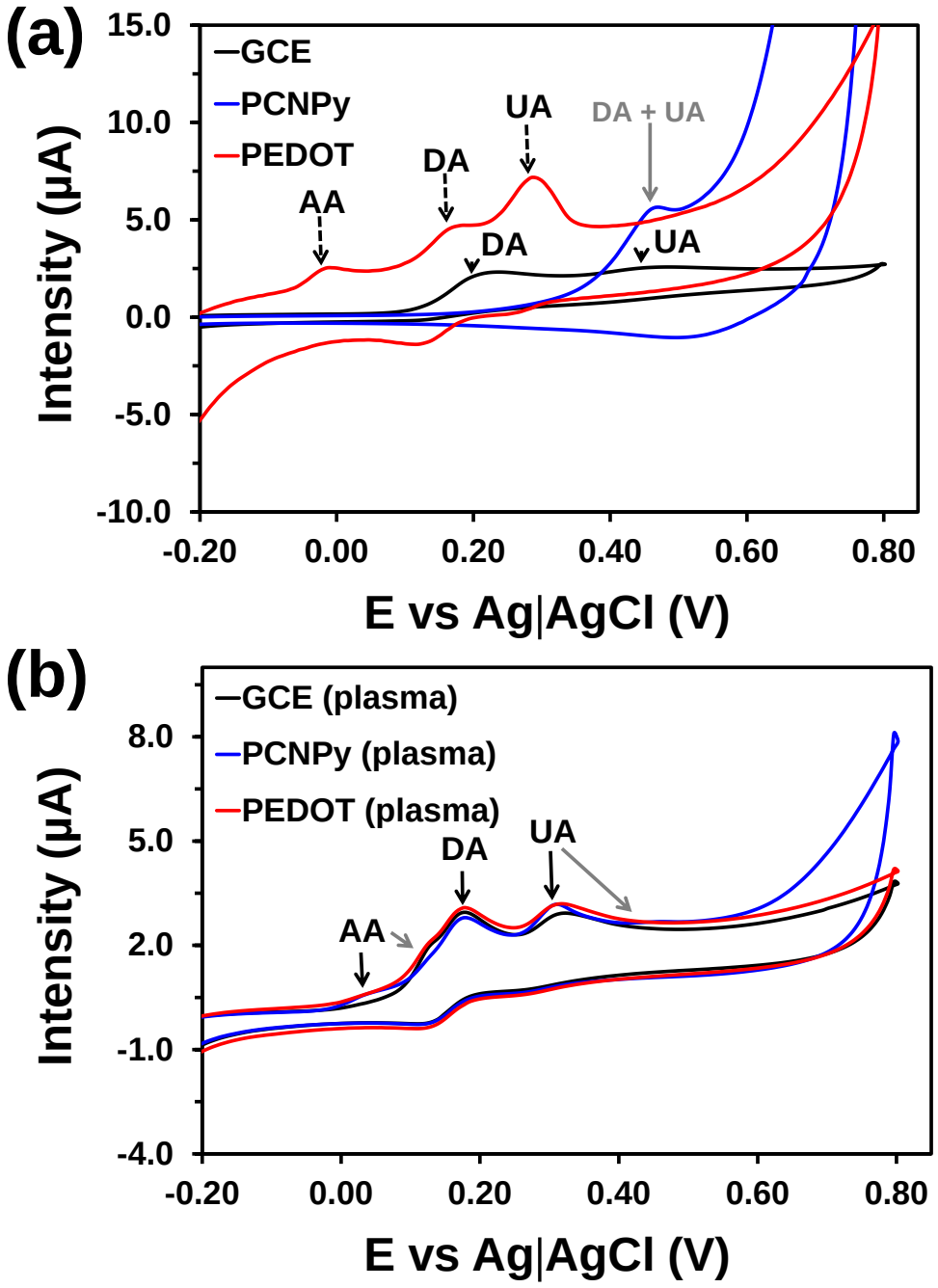
(a)
GCE
PCNPy
PEDOT
AA
DA
UA
DA + UA
DA
UA
Intensity (μA)
15.0
10.0
5.0
0.0
-5.0
-10.0
-0.20
0.00
0.20
0.40
0.60
0.80
E vs Ag|AgCl (V)
(b)
GCE (plasma)
PCNPy (plasma)
PEDOT (plasma)
AA
DA
UA
Intensity (μA)
8.0
5.0
2.0
-1.0
-4.0
-0.20
0.00
0.20
0.40
0.60
0.80
E vs Ag|AgCl (V)

Figure 1

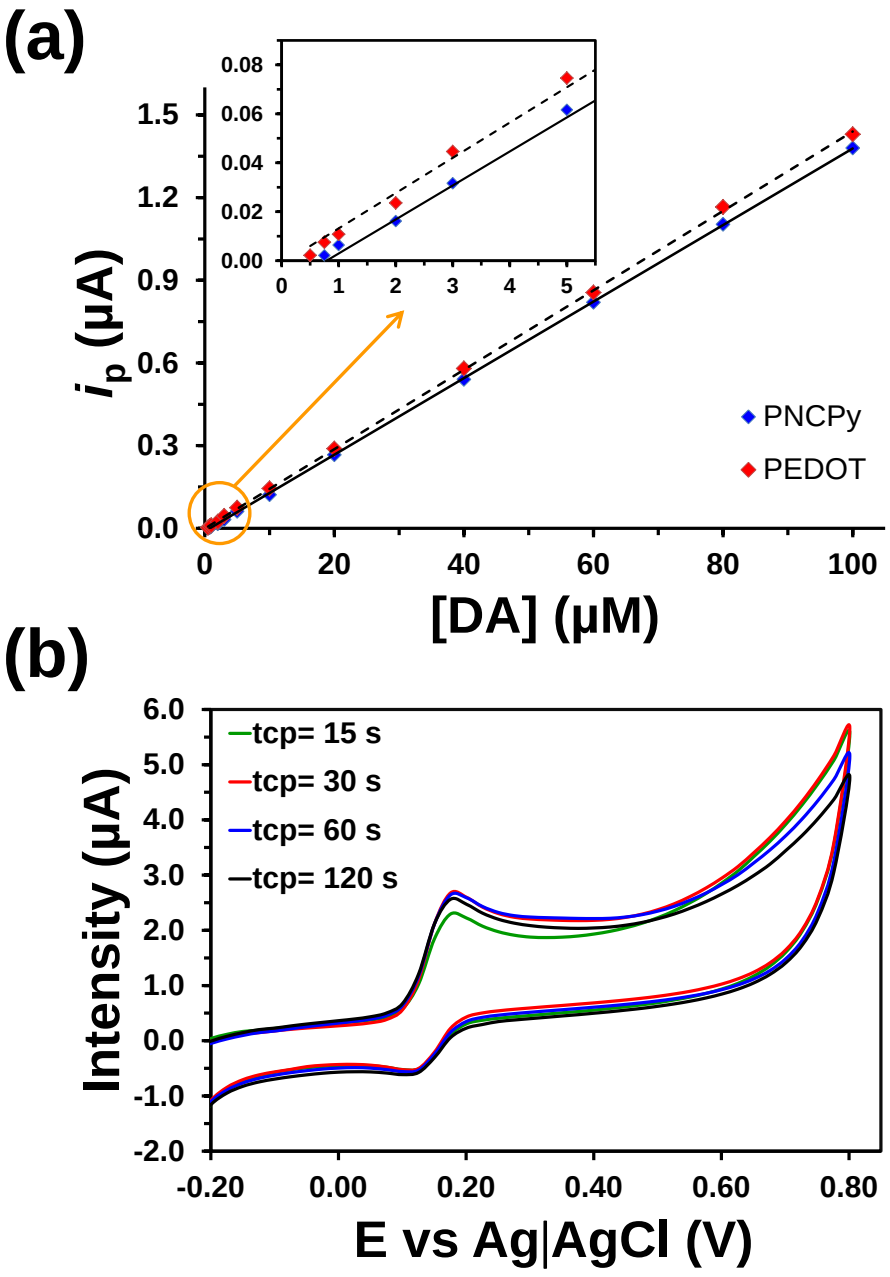
(a)
0.08
0.06
0.04
0.02
0.00
0
1
2
3
4
5
1.5
1.2
0.9
0.6
0.3
0.0
i_p (μA)
0
20
40
60
80
100
[DA] (μM)
PNCPy
PEDOT
(b)
6.0
5.0
4.0
3.0
2.0
1.0
0.0
-1.0
-2.0
Intensity (μA)
tcp= 15 s
tcp= 30 s
tcp= 60 s
tcp= 120 s
-0.20
0.00
0.20
0.40
0.60
0.80
E vs Ag|AgCl (V)

Figure 2

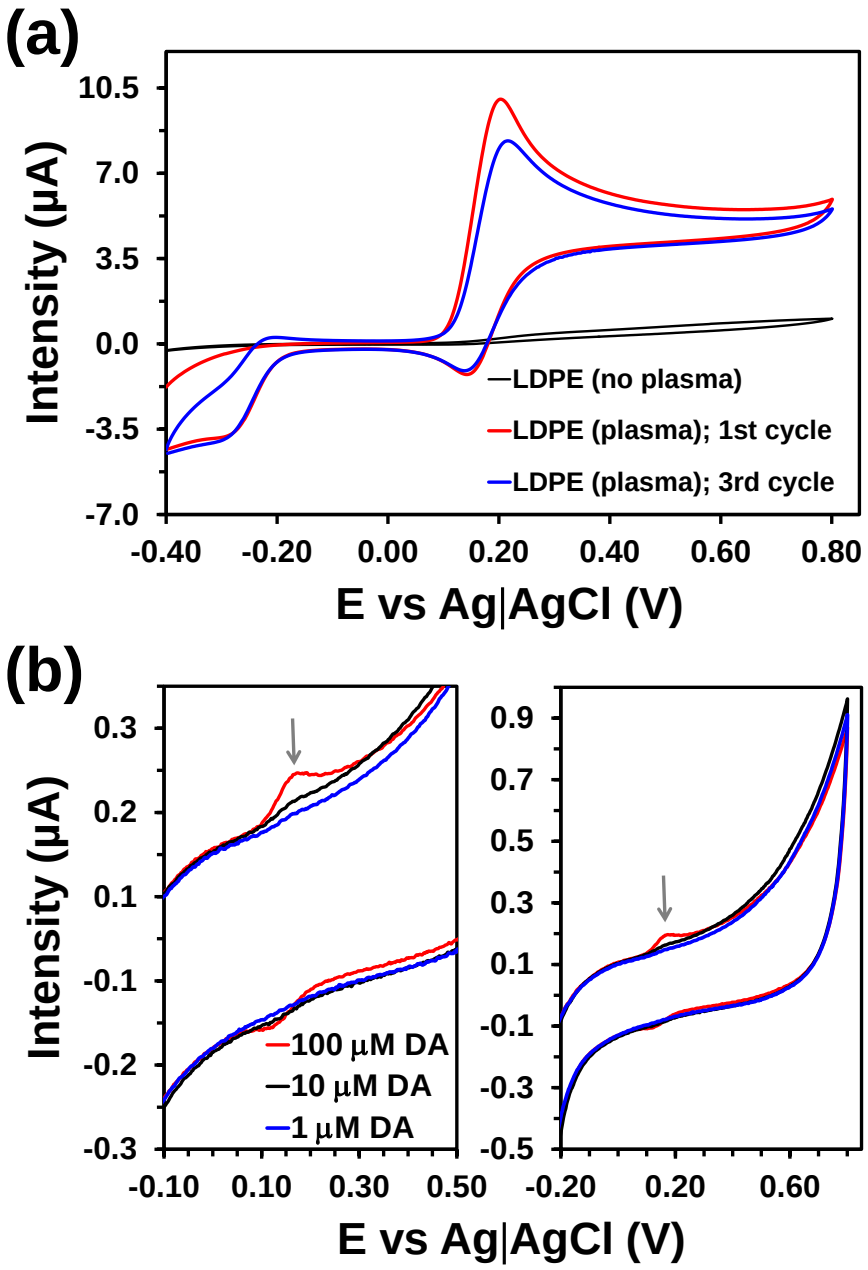
(a)
10.5
7.0
3.5
0.0
-3.5
-7.0
Intensity (μA)
-0.40
-0.20
0.00
0.20
0.40
0.60
0.80
E vs Ag|AgCl (V)
LDPE (no plasma)
LDPE (plasma); 1st cycle
LDPE (plasma); 3rd cycle
(b)
0.3
0.2
0.1
-0.1
-0.2
-0.3
Intensity (μA)
-0.10
0.10
0.30
0.50
0.9
0.7
0.5
0.3
0.1
-0.1
-0.3
-0.5
-0.20
0.20
0.60
E vs Ag|AgCl (V)
100 μM DA
10 μM DA
1 μM DA

Figure 3

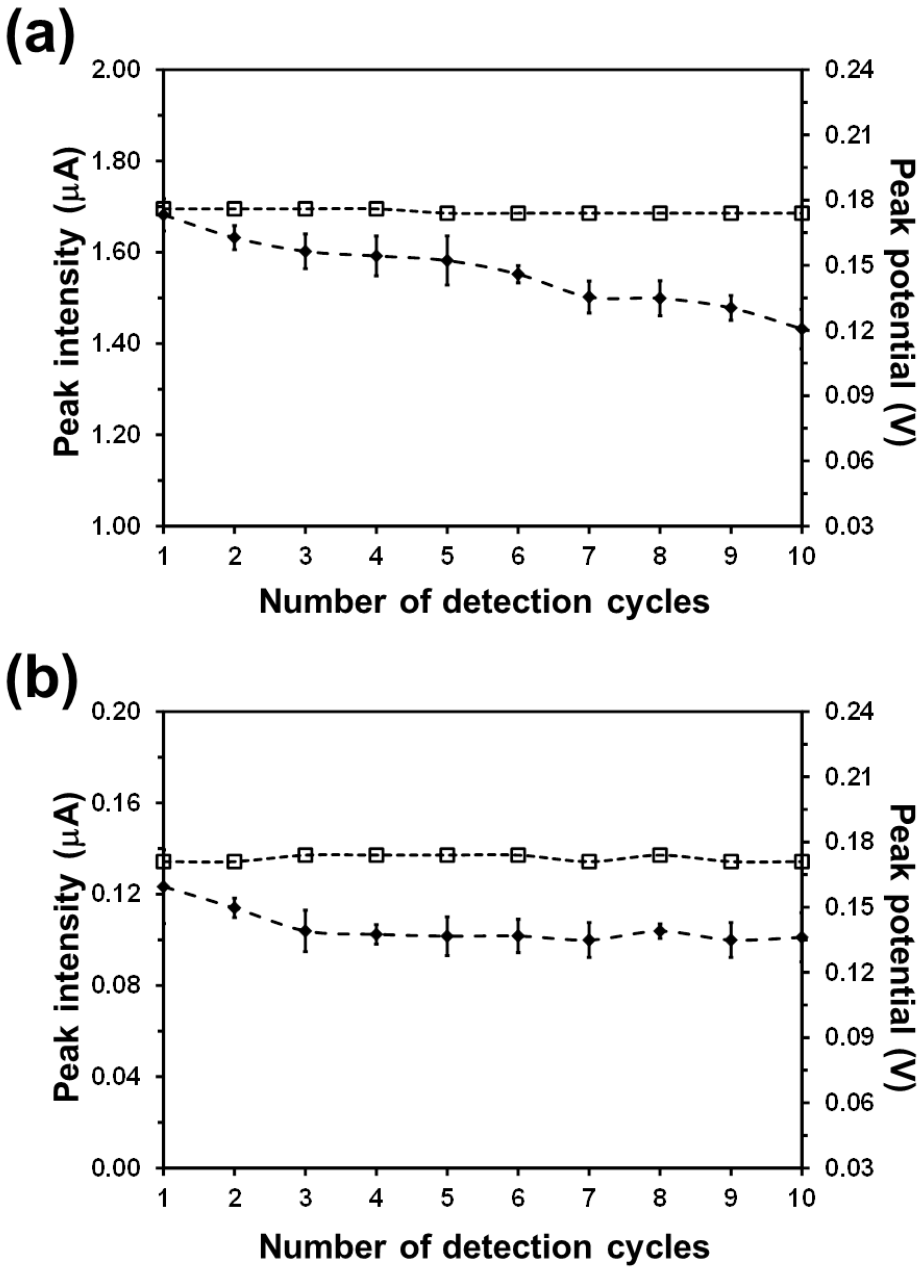
(a)
Peak intensity (μA)
Peak potential (V)
Number of detection cycles
(b)
Peak intensity (μA)
Peak potential (V)
Number of detection cycles

Figure 4

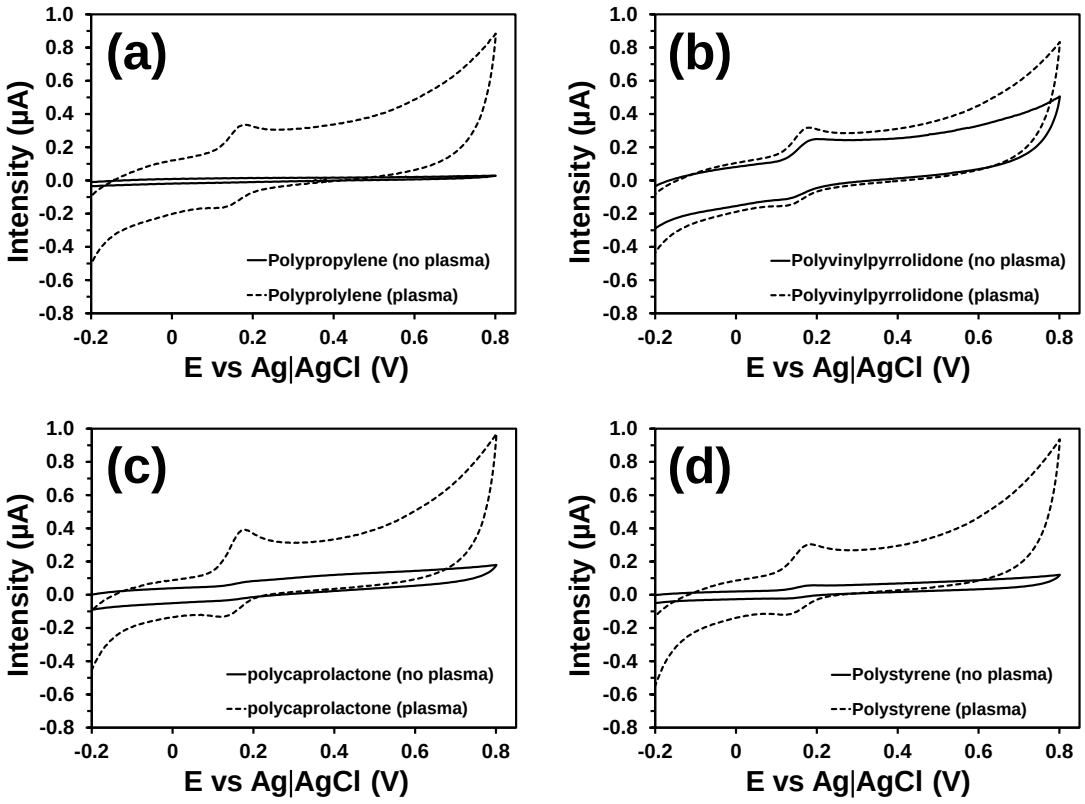
(a)
Intensity (µA)
E vs Ag|AgCl (V)
Polypropylene (no plasma)
Polyprolylene (plasma)
(b)
Intensity (µA)
E vs Ag|AgCl (V)
Polyvinylpyrrolidone (no plasma)
Polyvinylpyrrolidone (plasma)
(c)
Intensity (µA)
E vs Ag|AgCl (V)
polycaprolactone (no plasma)
polycaprolactone (plasma)
(d)
Intensity (µA)
E vs Ag|AgCl (V)
Polystyrene (no plasma)
Polystyrene (plasma)

Figure 5

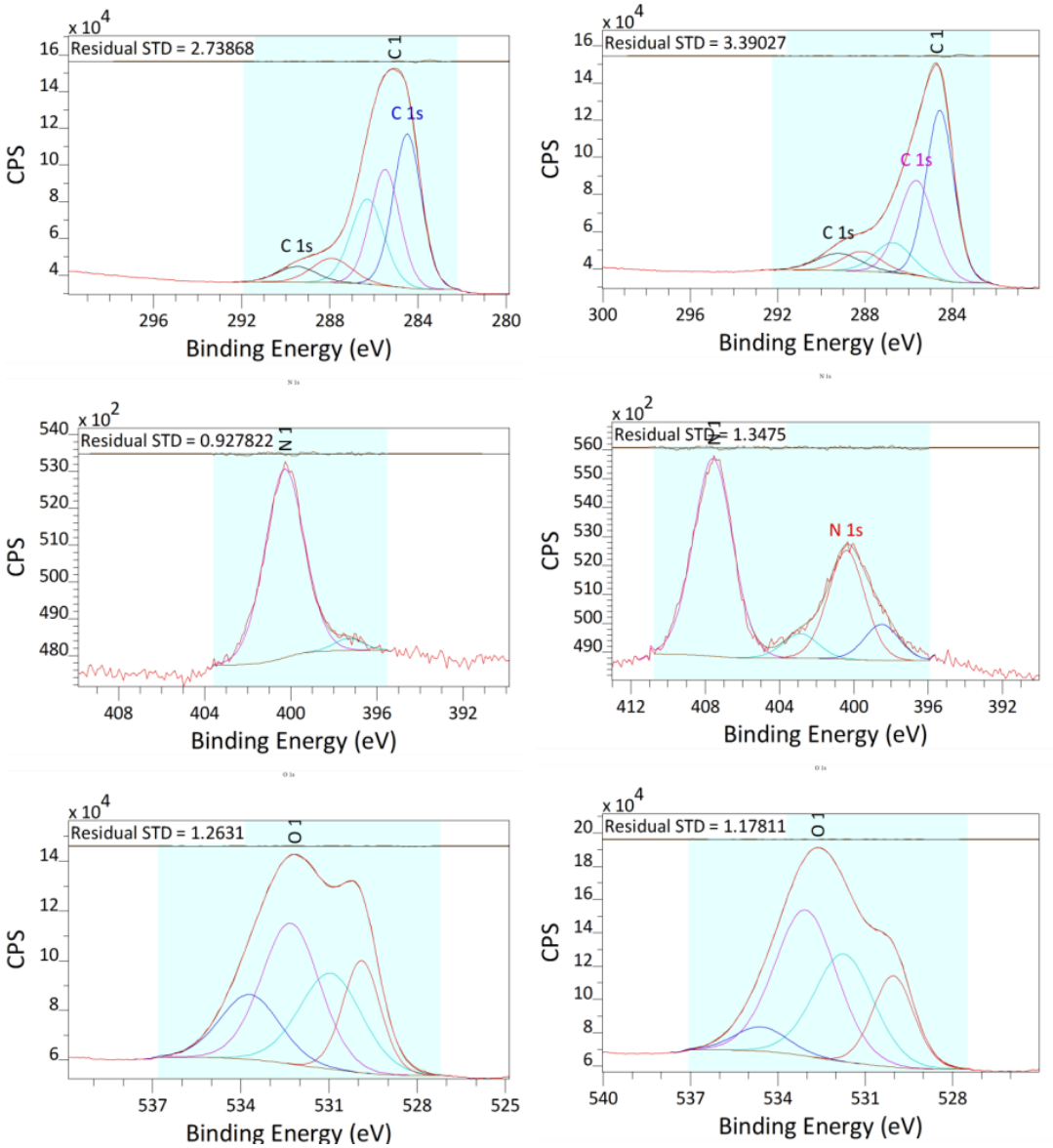
x 10^4
Residual STD = 2.73868
C 1
C 1s
C 1s
CPS
Binding Energy (eV)
x 10^4
Residual STD = 3.39027
C 1
C 1s
C 1s
CPS
Binding Energy (eV)
x 10^2
Residual STD = 0.927822
N 1
CPS
Binding Energy (eV)
x 10^2
Residual STD = 1.3475
N 1
N 1s
CPS
Binding Energy (eV)
x 10^4
Residual STD = 1.2631
O 1
CPS
Binding Energy (eV)
x 10^4
Residual STD = 1.17811
O 1
CPS
Binding Energy (eV)

Figure 6

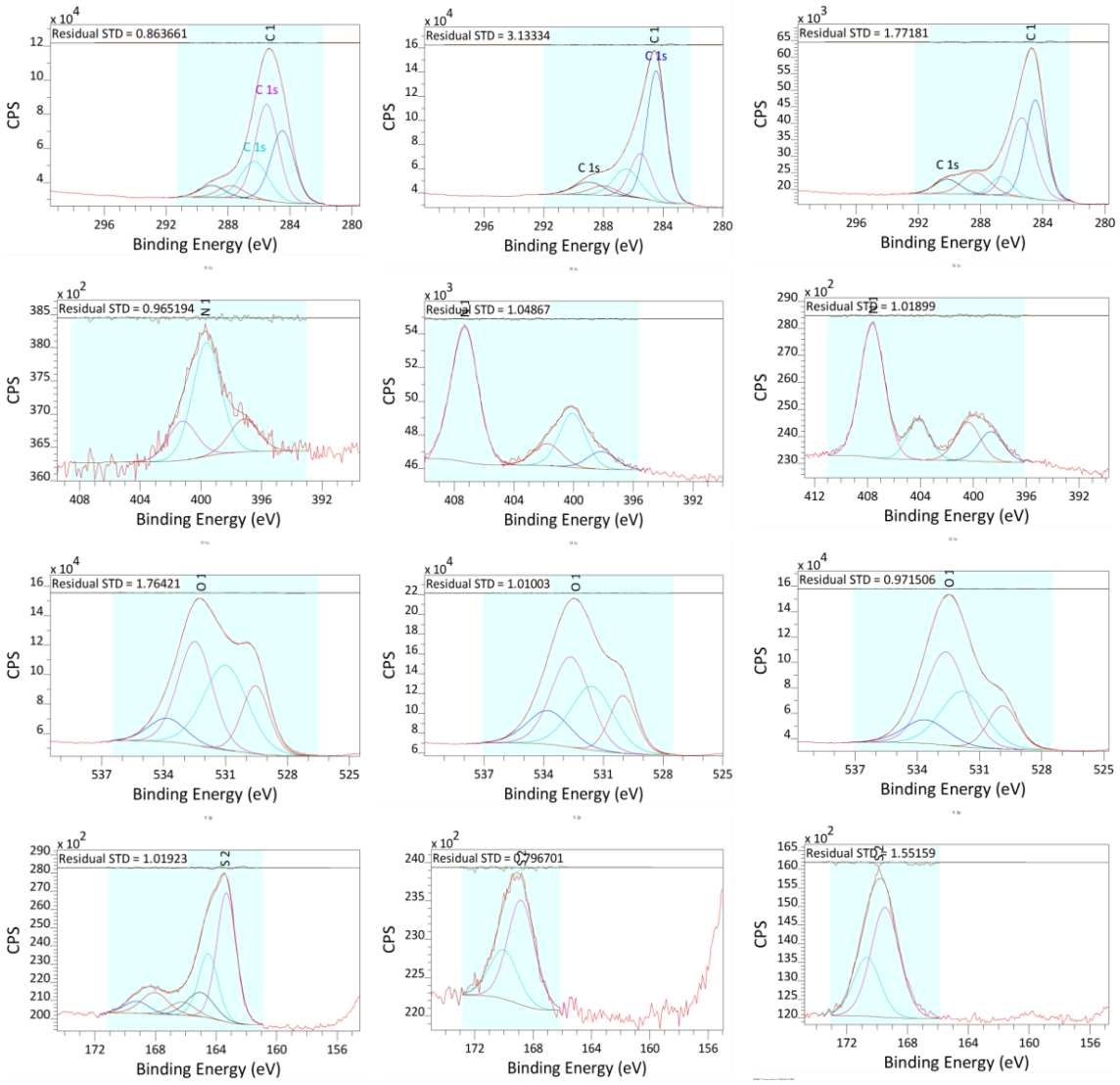
x 10^4
Residual STD = 0.863661
C 1
C 1s
C 1s
CPS
296 292 288 284 280
Binding Energy (eV)
x 10^4
Residual STD = 3.13334
C 1
C 1s
C 1s
CPS
296 292 288 284 280
Binding Energy (eV)
x 10^3
Residual STD = 1.77181
C 1
C 1s
CPS
296 292 288 284 280
Binding Energy (eV)
x 10^2
Residual STD = 0.965194
N 1
CPS
408 404 400 396 392
Binding Energy (eV)
x 10^3
Residual STD = 1.04867
N 1
CPS
408 404 400 396 392
Binding Energy (eV)
x 10^2
Residual STD = 1.01899
N 1
CPS
412 408 404 400 396 392
Binding Energy (eV)
x 10^4
Residual STD = 1.76421
O 1
CPS
537 534 531 528 525
Binding Energy (eV)
x 10^4
Residual STD = 1.01003
O 1
CPS
537 534 531 528 525
Binding Energy (eV)
x 10^4
Residual STD = 0.971506
O 1
CPS
537 534 531 528 525
Binding Energy (eV)
x 10^2
Residual STD = 1.01923
S 2
CPS
172 168 164 160 156
Binding Energy (eV)
x 10^2
Residual STD = 0.796701
CPS
172 168 164 160 156
Binding Energy (eV)
x 10^2
Residual STD = 1.55159
CPS
172 168 164 160 156
Binding Energy (eV)

Figure 7

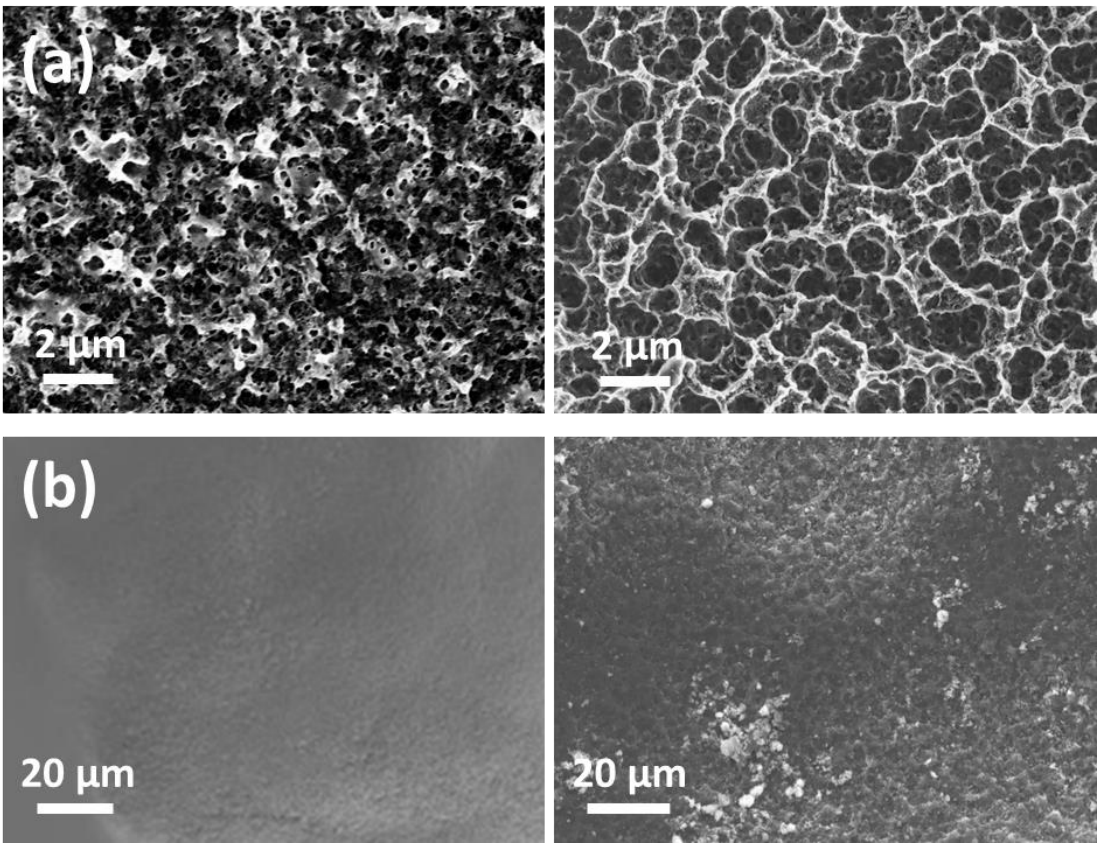

Figure 8

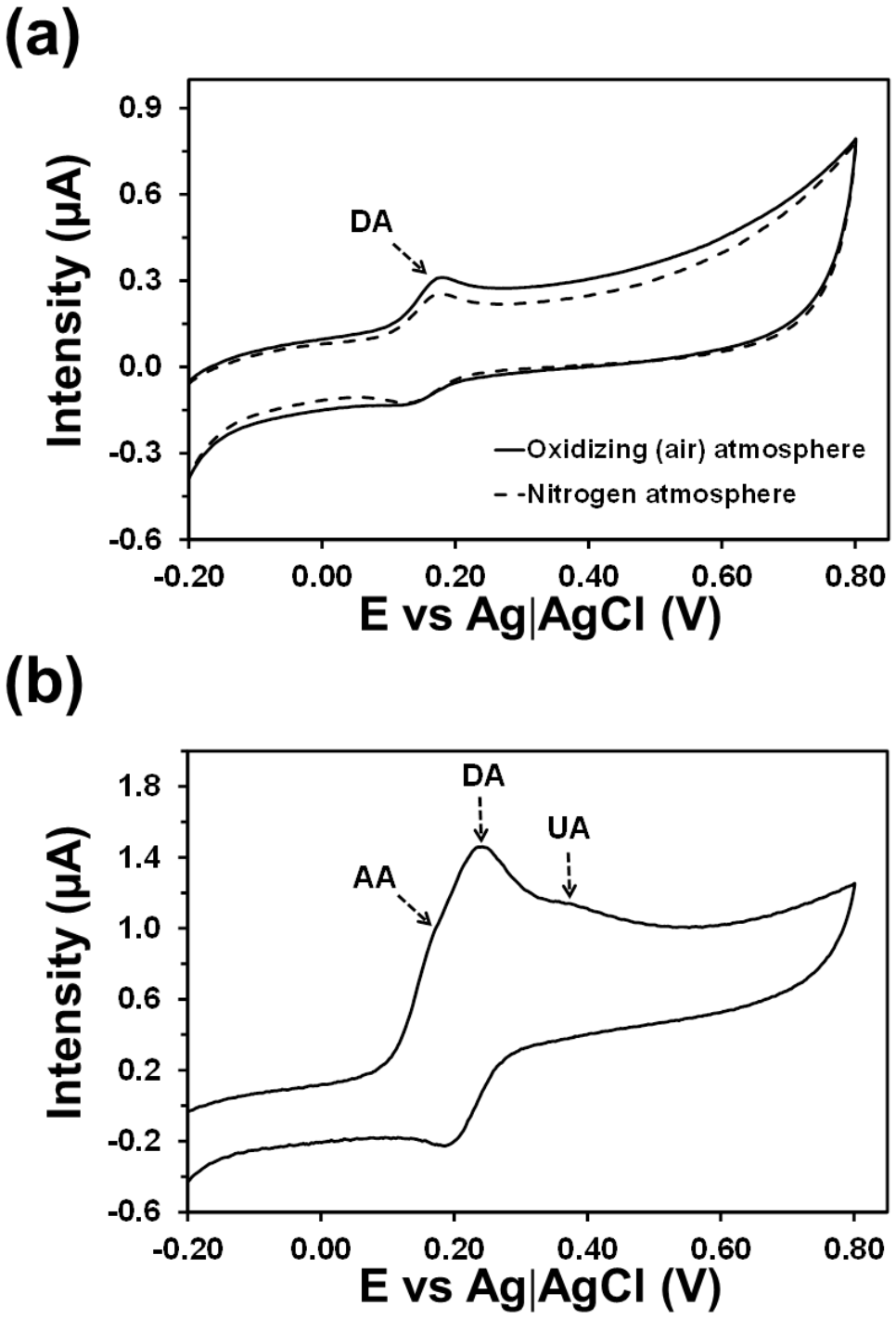
(a)
Intensity (μA)
0.9
0.6
0.3
0.0
-0.3
-0.6
DA
—Oxidizing (air) atmosphere
– -Nitrogen atmosphere
-0.20
0.00
0.20
0.40
0.60
0.80
E vs Ag|AgCl (V)
(b)
Intensity (μA)
1.8
1.4
1.0
0.6
0.2
-0.2
-0.6
DA
UA
AA
-0.20
0.00
0.20
0.40
0.60
0.80
E vs Ag|AgCl (V)

Figure 9

GRAPHICAL ABSTRACT